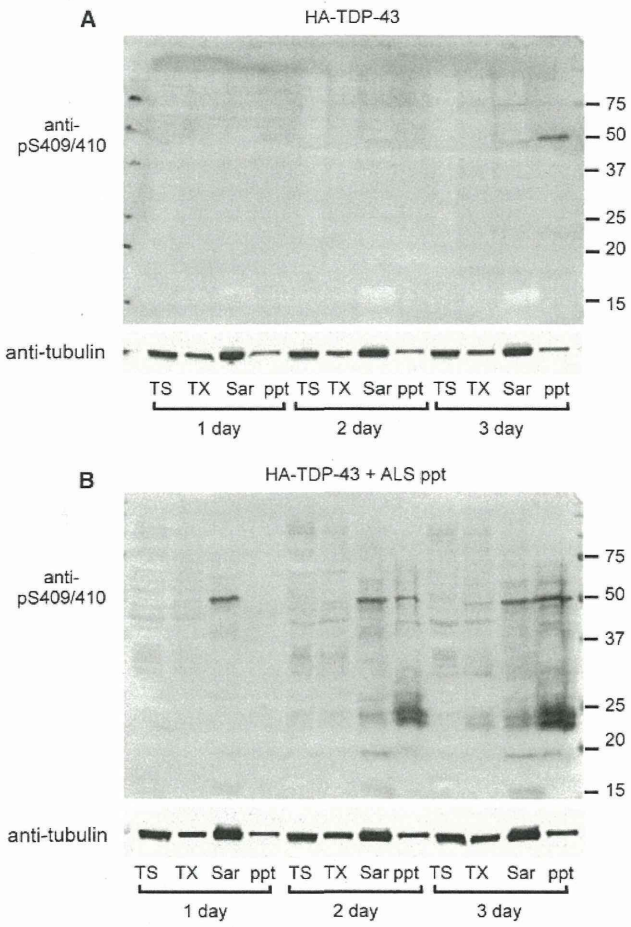

Figure 2. Time Course of Production of TDP-43 CTFs

(A and B) Cells transiently expressing HA-TDP-43 plasmid treated without (A) or with (B) ALS ppt were incubated for 1–3 days and then harvested. Proteins were differentially extracted and subjected to immunoblot analyses. Blots were probed with anti-pS409/410.

plasmid and ALS ppt, surprisingly, full-length HA-TDP-43 was accumulated even on day 1, whereas CTFs were not detected in any fraction at this time (Figure 2B). On and after day 2, not only full-length HA-TDP-43 but also CTFs were aggregated in cells. Thus, intracellular aggregation of full-length TDP-43 precedes generation of TDP-43 CTFs, suggesting that production of CTFs is not essential for formation of intracellular TDP-43 aggregates.

Characteristic CTFs of Insoluble TDP-43 in Each Disease Type Were Reproduced in a Self-Templating Manner in Cultured Cells

TDP-43 proteinopathy is classified into four types based on the predominant TDP-43-positive structures: type A mainly includes FTLD-TDP with GRN mutations, type B contains ALS and FTLD-MND, type C is representative of sporadic FTLD-TDP showing impairment of semantic memory, and type D refers to the pathology associated with inclusion body myopathy with early-onset Paget's disease and frontotemporal dementia caused by *VCP* mutations (Mackenzie et al., 2011). Each type is also characterized biochemically by the patterns of insoluble TDP-43 CTFs detected with anti-pS409/410 (Hasegawa et al., 2008; Tsuji et al., 2012). We prepared Sar-ppt from several types of brains (Figure 3A) and introduced them as seeds into cells expressing a plasmid encoding TDP-43. After 3 days of incubation, cells were harvested and each Sar-ppt was analyzed by immunoblotting with anti-pS409/410. In Figures 3A and 3B, all seeds prepared from TDP-43 proteinopathy brains (Nos. 1–8), but not from DLB (No. 9) or Pick's disease (No. 10) brain, were shown to function as seeds for TDP-43 aggregation in cultured cells, but the seeding efficiencies were different: type A and B seeds were more effective than type C. No sample was available from FTLD-TDP type D brain.

Next, to check whether each characteristic deposit of CTF was reproduced in cultured cells in the presence of each type of seed, we prepared insoluble fractions from TDP-43-expressing cells treated with seeds from each type of brain, and analyzed them by immunoblotting using anti-pS409/410. Interestingly, the band patterns of CTFs in the insoluble fraction (ppt) of cells expressing TDP-43 in the presence of each type of seed were different from each other, but quite similar to that of insoluble TDP-43 prepared as seeds from the corresponding patients (type A, B, or C), indicating that plasmid-derived TDP-43 is aggregated in a template-dependent manner in the presence of each type of seed (Figure 3C). These results suggest that seed-dependent TDP-43 aggregation, like prion aggregation, occurs in a self-templating manner. Insoluble TDP-43 from diseased brains appears to have features similar to those of pathogenic prion.

Insoluble TDP-43 Has Prion-like Properties

Next, we examined whether insoluble TDP-43 from brains of patients has prion-like characteristics. First, we tested whether detergent-insoluble TDP-43 prepared from cells containing TDP-43 aggregates as well as seeds from brains can promote intracellular TDP-43 aggregation. Triton X-100 (TX)-insoluble fraction was prepared as seeds from cells containing aggregates (Figure 4A, right panel) and introduced into cells. In a control experiment, we confirmed that insoluble seeds from cells expressing HA-TDP-43 treated with ALS ppt (HA-TDP-43+ALS ppt) did not serve efficiently as seeds for endogenous TDP-43 aggregation (Figure S3A). In cells expressing HA-TDP-43 and treated with TX-insoluble seeds from cells transfected with both HA-TDP-43 and ALS ppt, phosphorylated full-length HA-TDP-43 and CTFs were observed in the insoluble fraction (ppt; Figure 4A), whereas the band of phosphorylated full-length HA-TDP was hardly detectable in the insoluble fraction from cells expressing HA-TDP-43 and treated with TX-insoluble seed from cells without transfection (none) or treated with TX-insoluble seed from cells expressing HA-TDP-43 alone (HA-TDP-43). In immunocytochemical analyses of cells expressing HA-TDP-43 and treated with TX-insoluble seeds from cells transfected with both HA-TDP-43 and ALS ppt (HA-TDP-43+ALS ppt), we observed inclusions positive for both anti-pS409/410 and anti-Ub (Figure 4B), which were very similar to those observed in cells expressing

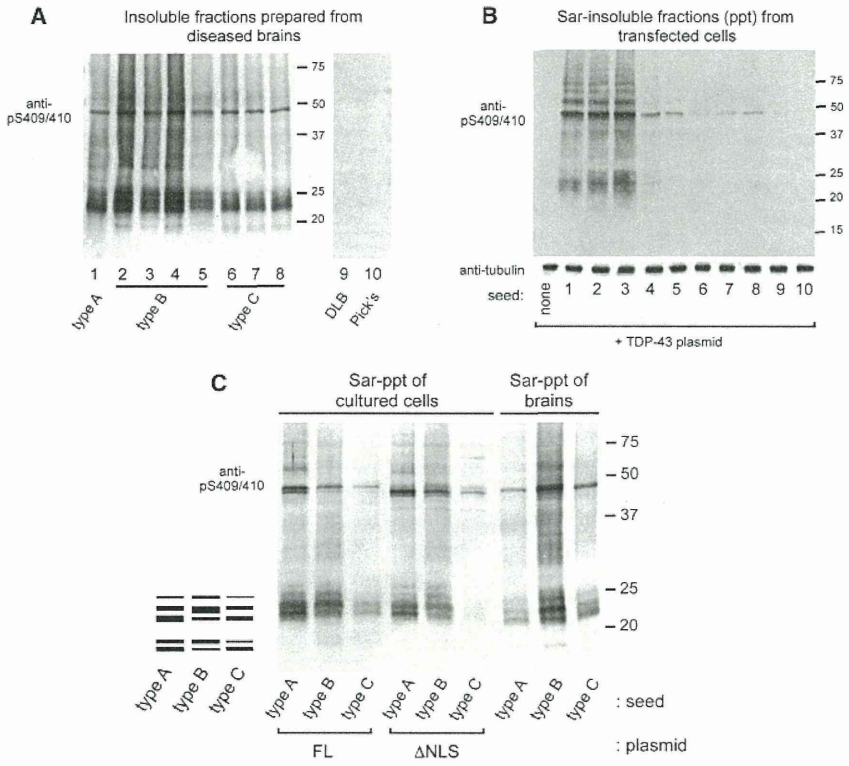

Figure 3. Formation of Self-Templating Aggregates Induced by Insoluble TDP-43 from the Brains of Patients

(A) Immunoblot analyses of Sar-ppt prepared from several diseased brains used as seeds.

(B) Immunoblot analyses of Sar-ppt of cells expressing TDP-43 treated with each seed (Nos. 1–10).

(C) Comparison of band patterns of Sar-ppt fractions from cells expressing full-length TDP-43 (FL) or TDP-43 lacking nuclear localization signal (78–84 residues: ΔNLS) treated with type A, B, or C seed. Sar-ppt fractions from each of the diseased brains are shown next to cellular ppt fractions on the same blot. A schematic diagram of the band pattern of TDP-43 CTFs is also presented. Blots were probed using anti-pS409/410.

HA-TDP-43 treated with ALS ppt (Figure 1E). These results indicate that TX-insoluble seeds produced from cells containing TDP-43 aggregates can function as seeds for further aggregation of TDP-43.

We also checked the effects of heat treatment or proteinase digestion of insoluble TDP-43 on seeding ability. Each type of seed was treated or not treated at 100°C for 5 min (boiling) and analyzed by immunoblotting with anti-pS409/410. No marked differences in the band patterns of each type of seed were seen before or after the boiling treatment (Figure 4C, left panel). Then, these seeds were introduced into TDP-43-expressing cells, and Sar-ppts prepared from the cells were analyzed by immunoblotting with anti-pS409/410 (Figures 4C and S3B). In the case of type A seed, the seeding effect on TDP-43 aggregation was unaffected by boiling, whereas the ability of type B and C seeds to induce TDP-43 aggregation was almost abrogated after boiling (Figure 4C, middle and right panels). All of these seeds were easily degraded into <20 kDa CTFs by Proteinase K (ProK) treatment (Figure 4D, left panel). However, seeding ability to induce intracellular TDP-43 aggregation was retained even after ProK digestion (Figure 4D, middle and right panels, and Figure S3C).

Furthermore, we tested whether formic acid, which destroys the β-sheet structure of proteins, influences the seeding ability of insoluble TDP-43. As shown in Figures 4E, S3D, and S3E, insoluble fractions from type A, B, and C brains treated with formic acid did not induce intracellular TDP-43 aggregation, suggesting that β-sheet-rich structure is necessary for seeding activity. Taken together, these results show that insoluble TDP-43 has prion-like properties, including repeated seeding ability and sensitivity to heat, proteinase, or formic acid.

Intracellular Aggregate Formation of TDP-43 Induces Cell Death in Cultured Cells

To examine whether intracellular TDP-43 aggregates cause neuronal dysfunction leading to cell death, we measured the rate of cell death in cells containing intracellular TDP-43 aggregates by means of lactate dehydrogenase (LDH) assay. Cells transfected with TDP-43 were treated with insoluble fractions from TDP-43 proteinopathy brains or Pick's disease brain and incubated for 3 days, followed by LDH assay. As shown in Figure 5A, the rate of cell death was almost 5% in cells treated only with insoluble fractions from type B or plasmid transfection, whereas it was ~20% in cells expressing TDP-43 and treated with each TDP-43 proteinopathy brain extract. These cell lysates were also analyzed by immunoblotting. Increased cell death of these cells was accompanied by deposition of phosphorylated TDP-43 in the Sar-ppt fraction (Figure 5B). However, no significant cell death was observed in cells expressing TDP-43 and treated with Pick's disease brain extract, in which phosphorylated TDP-43 was not deposited. These results suggest that increased cell death of cells containing TDP-43 aggregates is correlated with the amount of intracellular TDP-43 aggregates.

Intracellular Accumulation of TDP-43 Aggregates Elicits Proteasome Dysfunction

Previously, we reported that proteasome activity was suppressed in cells containing intracellular α-synuclein aggregates (Nonaka et al., 2010). To examine whether intracellular aggregates of TDP-43 also induce proteasome dysfunction, we assayed proteasome activity in cells containing TDP-43 aggregates by using the GFP-CL1 reporter (Bence et al., 2001), which is available to monitor proteasome activity in cultured cells (Nonaka and Hasegawa, 2009; Nonaka et al., 2010).

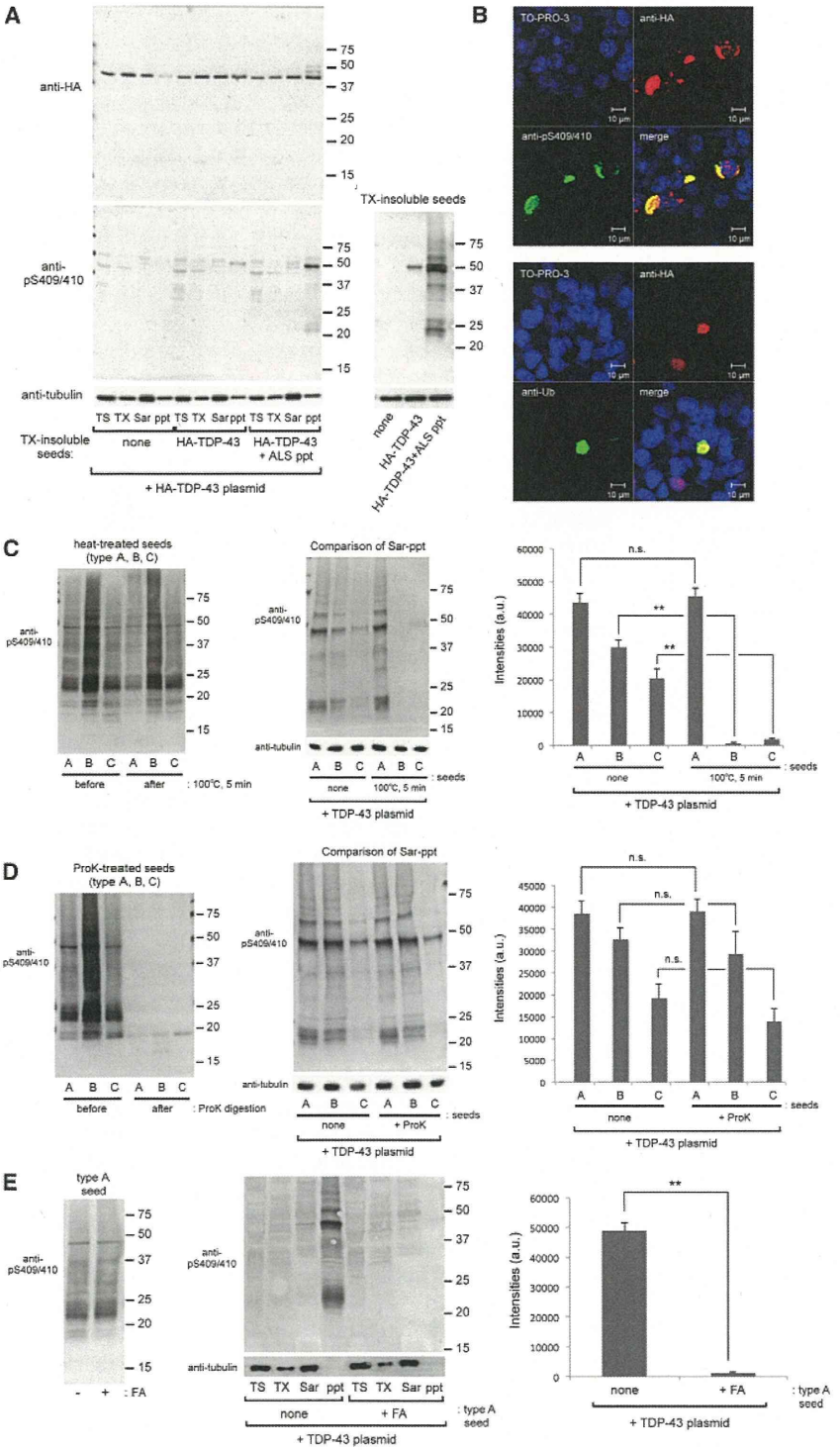

Figure 4. Characterization of the Prion-like Properties of Detergent-Insoluble TDP-43 from Brains

(A) Immunoblot analyses of cells expressing HA-TDP-43 and treated with Triton X-100-insoluble fractions (TX-insoluble seeds) prepared from the following cells, using anti-HA (upper) and anti-pS409/410 (lower): none, mock cells; HA-TDP-43, cells expressing HA-TDP-43; and HA-TDP-43+ALS ppt, cells expressing HA-TDP-43 and treated with ALS ppt. These TX-insoluble seeds (10 μg each) were also immunoblotted with anti-pS409/410 (lower right).

(B) Confocal laser microscopy analyses of cells expressing HA-TDP-43 and treated with TX-insoluble seed from cells transfected with both HA-TDP-43 and ALS ppt (HA-TDP-43+ALS ppt) immunostained with anti-HA (red), anti-pS409/410 (green), or anti-Ub (green), and counterstained with TO-PRO-3 (blue). Scale bars: 10 μm.

(C) Effect of heat treatment on the seeding ability of each type of seed. Each seed before and after heat treatment (100°C for 5 min) was analyzed by immunoblotting using anti-pS409/410 (left). Then, cells expressing TDP-43 were treated with these fractions as seeds. After 3 days of incubation, Sar-ppt fractions were prepared and analyzed by immunoblotting using anti-pS409/410 (middle). The immunoreactivity of each lane that was positive for anti-pS409/410 was quantified and the results are expressed as means + SEM (n = 3). **p < 0.0001 by Student's t test; n.s., not significant; a.u., arbitrary unit. See also Figure S3.

(D) Effect of ProK on the seeding ability of each type of seed. Each seed before and after ProK digestion (final 20 μg/mL ProK at 37°C for 30 min) was analyzed by immunoblotting using anti-pS409/410 (left). Then, cells expressing TDP-43 were treated with these fractions as seeds. After 3 days of incubation, the Sar-ppt fractions were analyzed by immunoblotting using anti-pS409/410 (middle). The immunoreactivity of each lane that was positive for anti-pS409/410 was quantified and the results are expressed as means + SEM (n = 3). n.s., not significant; a.u., arbitrary unit. See also Figure S3.

(E) Effect of formic acid (FA) on the seeding ability of type A seed. Type A seed with or without FA treatment was analyzed by immunoblotting using anti-pS409/410 (left). Then, cells expressing TDP-43 were treated with these fractions as seeds. After 3 days of incubation, fractionated samples were analyzed by immunoblotting using anti-pS409/410 (right). The immunoreactivity of ppt fractions that were positive for anti-pS409/410 was quantified and the results are expressed as means + SEM (n = 3). **p < 0.0001 by Student's t test. a.u., arbitrary unit. See also Figure S3.

Cells were transfected with TDP-43 and GFP-CL1 plasmids overnight, followed by transduction of ALS ppt. After 3 days of incubation, the cells were analyzed by confocal microscopy and immunoblotting. As shown in Figures 6A and 6B, GFP fluorescence in cells transfected with GFP-CL1 alone was very low due to degradation of GFP-CL1 by proteasome. When cells expressing GFP-CL1 were treated with proteasome inhibitor MG132 (0.1 μM), GFP fluorescence intensity

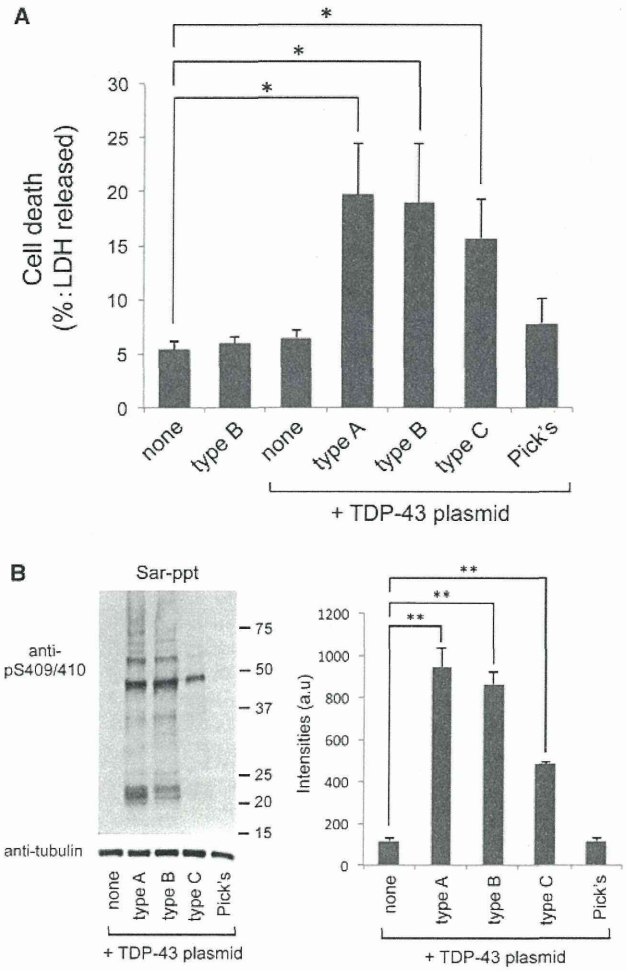

Figure 5. Cell Death Induced by the Formation of Intracellular TDP-43 Aggregates

(A) The extent of cell death of transfected cells was quantified by an LDH release assay. Cells treated with type B seed alone (type B), cells transfected with TDP-43 plasmid alone, or cells expressing TDP-43 and treated with Sar-ppt from type A, B, or C, or Pick's disease brains were cultured, and a cell death assay was performed 3 days thereafter. The results are expressed as means + SEM (n = 5). *$p < 0.05$ versus "none" by Student's t test.

(B) Immunoblot analyses of Sar-ppt from cells expressing TDP-43 and treated with extracts of type A, B, C, and Pick's disease brains, using anti-pS409/410. Immunoreactivity to anti-pS409/410 was quantified in each lane. The results are expressed as means + SEM (n = 3). **$p < 0.001$ versus "none" by Student's t test. a.u., arbitrary unit.

was significantly higher. GFP fluorescence in cells transfected with TDP-43 alone or treated with ALS ppt alone was as low as that in cells expressing only GFP-CL1, whereas it was significantly higher in cells expressing TDP-43 and treated with ALS ppt. We confirmed that cells containing phosphorylated TDP-43 aggregates were strongly positive for GFP (Figure 6C). These results suggest that proteasome activity is suppressed in cells harboring intracellular TDP-43 aggregates.

Phosphorylated TDP-43 Aggregates Are Propagated between Cultured Cells

To examine whether TDP-43 aggregates can be transferred between cultured cells, we performed coculture experiments. SH-SY5Y cells expressing only DsRed were cocultured with SH-S5Y5 cells harboring phosphorylated TDP-43 aggregates in a 1:1 ratio. After incubation for 3 days, the cells were stained with anti-pS409/410 and analyzed by confocal laser microscopy. The presence of phosphorylated TDP-43 aggregates immunolabeled with Alexa-488 in cells expressing DsRed would indicate that phosphorylated TDP-43 aggregates could spread to cells that originally did not contain these aggregates. As shown in Figures 7A and 7B, phosphorylated TDP-43 aggregates (green) were found in the cytoplasm of cells expressing DsRed. The percentage of DsRed-positive cells that also contained phosphorylated TDP-43 aggregates was calculated to be 2.9% ± 0.8%. In three-dimensional image modeling of a DsRed-expressing cell with TDP-43 aggregates, the signal of phosphorylated TDP-43 aggregates was merged with that of DsRed in the X-Z and Y-Z cross-sections (Figure 7B).

Next, we examined how TDP-43 aggregates are released from cells. It has been hypothesized that protein aggregates are released via exosome (Fevrier et al., 2004; Goedert et al., 2010). To investigate whether this mechanism operates for TDP-43 aggregates, we prepared exosome fractions from cells expressing TDP-43 plasmid alone, cells treated with ALS ppt alone, or cells expressing TDP-43 and treated with ALS ppt using the ExoQuick-TC kit (SBI). Immunoblot analyses showed that in cells expressing TDP-43 and treated with ALS ppt, the band intensity of full-length TDP-43 in the exosome fraction was significantly increased as compared with that in cells transfected with TDP-43 plasmid or ALS ppt alone (Figure 7C), whereas expression of the exosome marker protein CD63 was similar in all of the exosome fractions. These results suggest the possibility that exosome may contribute to the release of intracellular TDP-43 aggregates.

DISCUSSION

Prion-like propagation of aggregated proteins in neurodegenerative diseases is well established (Clavaguera et al., 2009; Desplats et al., 2009; Frost et al., 2009; Goedert et al., 2010; Kordower et al., 2008; Li et al., 2008; Luk et al., 2009; Nonaka et al., 2010; Masuda-Suzukake et al., 2013; Polymenidou and Cleveland, 2011; Ren et al., 2009). Here, we show that insoluble TDP-43 prepared from TDP-43 proteinopathy brains (type A, B, and C) can function as seeds for intracellular TDP-43 aggregation in cultured cells. Type A, B, and C brains showed distinct banding patterns of TDP-43 CTFs in immunoblot analyses with anti-pS409/410 (Hasegawa et al., 2008; Tsuji et al., 2012). The band patterns of characteristic CTFs are thought to reflect structural differences of TDP-43 fibrils deposited in each type of brain (Hasegawa et al., 2008; Tsuji et al., 2012). Interestingly, band patterns of CTFs characteristic of the individual seeds were seen in intracellular TDP-43 aggregates in cultured cells, indicating that plasmid-derived TDP-43 aggregation occurs in a self-templating manner. The seeding activity of insoluble TDP-43 from patients' brains was stable against detergents, heat

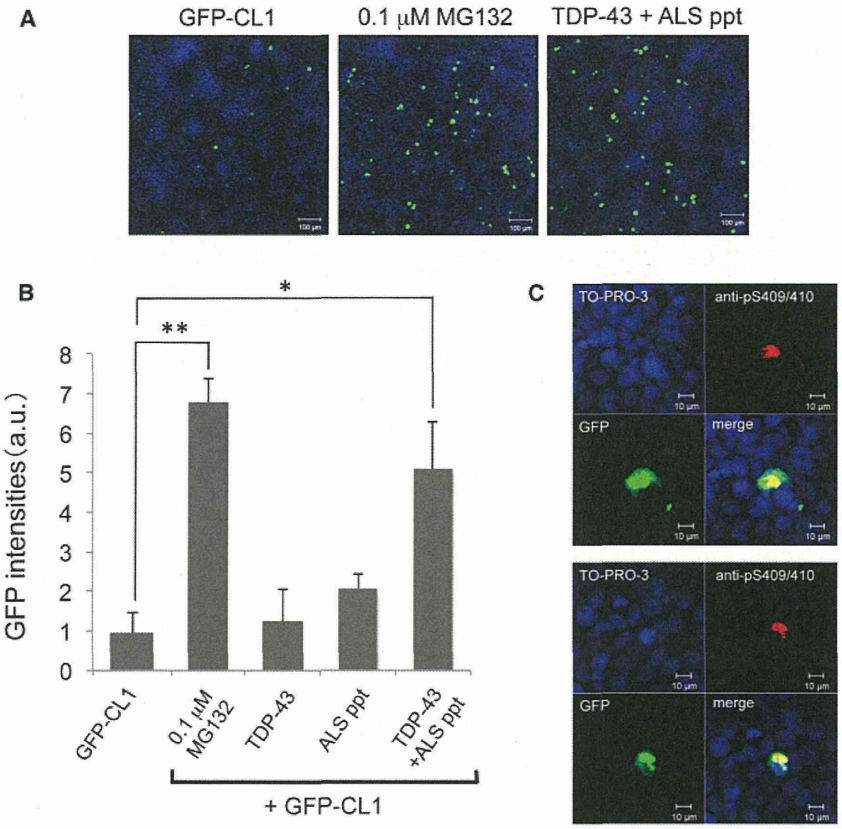

Figure 6. Proteasome Dysfunction in Cells Bearing Intracellular TDP-43 Aggregates

(A–C) SH-SY5Y cells transfected with both GFP-CL1 and TDP-43 were treated with ALS ppt for 2 days.

(A) As a control, cells expressing GFP-CL1 with or without 0.1 μM MG132 or ALS ppt, and cells expressing both GFP-CL1 and TDP-43 were also analyzed.

(B) The intensity of GFP fluorescence in these cells was quantified. The results are expressed as means + SEM (n = 3). *$p < 0.05$; **$p < 0.001$ versus the value of GFP-CL1 by Student's t test. a.u., arbitrary unit.

(C) Cells transfected with both GFP-CL1 and TDP-43 and treated with ALS ppt were stained with anti-pS409/410.

treatment, or proteolytic digestion, and cell-to-cell transmission ability was retained. Formic acid abrogated the seeding ability, suggesting that β-sheet structure in insoluble TDP-43 is indispensable for this ability. Thus, insoluble TDP-43 in the brains of patients has the characteristics of a pathogenic prion, suggesting that TDP-43 proteinopathy involves mechanisms similar to those of prion disease. It remains unclear, however, how protein aggregates spread between cells in vivo. It seems likely that prion-like aggregates are released from cells and taken up by neighboring cells, where they penetrate the cytoplasm and act as nuclei for further aggregation (Goedert et al., 2010). Prions are transferred between cultured cells via exosomes or tunneling nanotubes (Fevrier et al., 2004; Gousset et al., 2009), and our results indicate that TDP-43 aggregates may also be transferred from cell to cell at least partly via exosomes. Further investigation is needed to elucidate in detail the mechanisms of intercellular propagation of protein aggregates in vitro and in vivo. Nevertheless, taken together, our data suggest that TDP-43 proteinopathy can be classified as a prion disease.

Phosphorylated TDP-43 CTFs, as well as phosphorylated full-length TDP-43, are deposited in affected neurons in TDP-43 proteinopathy (Hasegawa et al., 2008, 2011). TDP-43 CTFs identified in FTLD-TDP brains are more prone to form aggregates than the full-length molecule in cultured cells (Igaz et al., 2009; Nonaka et al., 2009). Further, they bind with full-length TDP-43 and may facilitate aggregation of full-length TDP-43 in cultured cells (Budini et al., 2012; Nonaka et al., 2009; Zhang et al., 2009). Therefore, generation of pathogenic TDP-43 CTFs may be crucial for the formation of intracellular TDP-43 inclusions leading to neuronal cell death. However, our time-course immunoblotting analyses (Figure 2) showed that full-length TDP-43 aggregation preceded the deposition of CTFs, suggesting that cleavage of TDP-43 to produce CTFs is not a trigger for intracellular TDP-43 aggregate formation. Thus, it appears that the generation of CTFs is a consequence of degradation of phosphorylated full-length TDP-43 to eliminate abnormal and toxic aggregates of TDP-43, rather than a cause of aggregation of full-length TDP-43. In other words, TDP-43 CTFs deposited in affected neurons represent the residual stable core portion of TDP-43 aggregates left after degradation by intracellular proteolytic systems.

Abnormal posttranslational modifications and abnormal structure of seeds for aggregation are important for reproducing the pathological and biochemical features of TDP-43 inclusions found in the brains of patients with TDP-43 proteinopathy in cultured cells. Indeed, intracellular TDP-43 aggregates obtained using recombinant TDP-43 fibrils as seeds appeared as very small dot-like structures without phosphorylation (Furukawa et al., 2011), and were quite different from the TDP-43 inclusions found in the brains of patients. Our model for seeded aggregation of TDP-43 seems consistent with the pathological and biochemical changes found in the brains of patients with TDP-43 proteinopathy: in the model, aggregated TDP-43 is phosphorylated and ubiquitinated, and immunoreactivity of TDP-43 in nuclei of cells containing cytoplasmic TDP-43 aggregates is relatively weak. We also observed significant cell death and proteasome dysfunction associated with the presence of intracellular TDP-43 aggregates. It is possible that such proteasome dysfunction is caused by overloading of the ubiquitin-proteasome system with ubiquitinated proteins, including TDP-43 aggregates. The resulting suppression of proteasome activity might induce cell death. We previously observed a similar phenomenon (Nonaka et al., 2010); i.e., seed-dependent intracellular

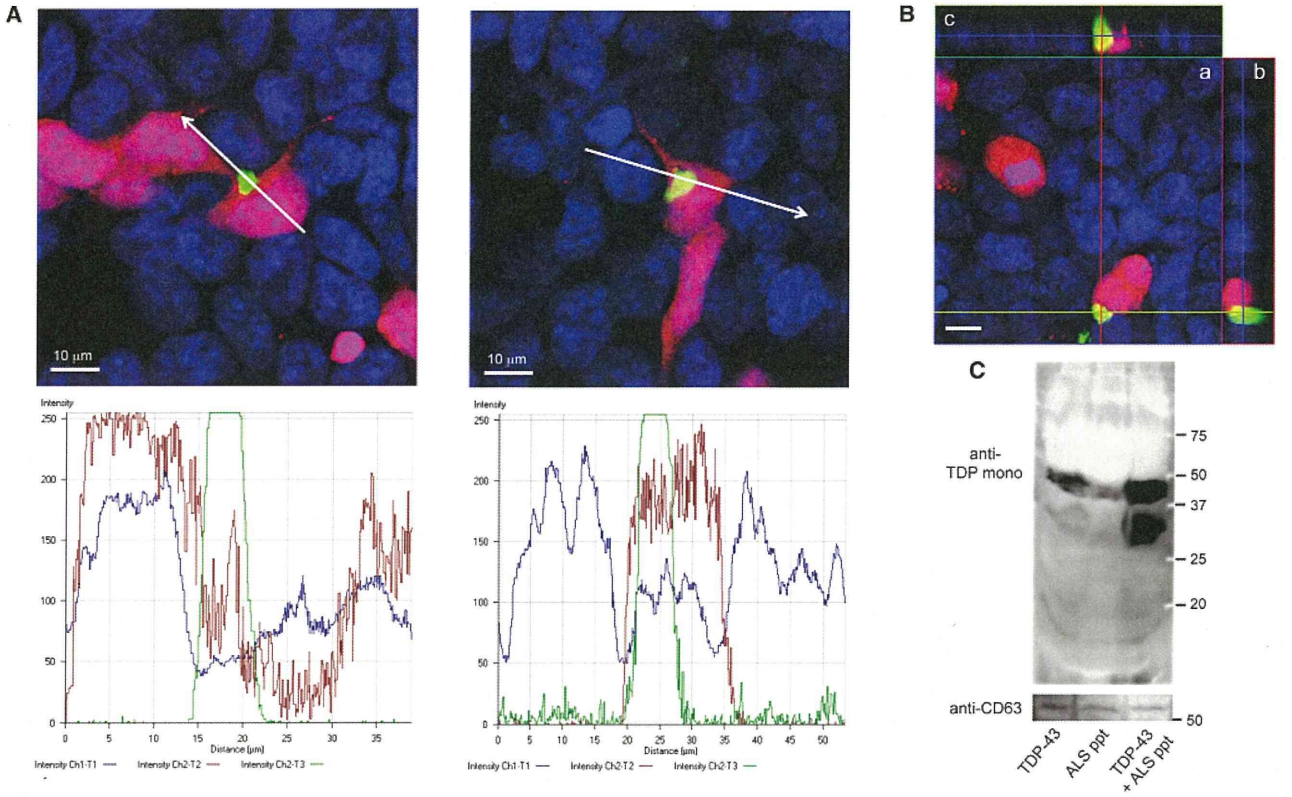

Figure 7. Intracellular TDP-43 Aggregates Are Released in Association with Exosome

(A) Coculture of cells expressing DsRed and cells having intracellular TDP-43 aggregates in a 1:1 ratio. After incubation for 3 days, cells were stained with pS409/410 (green) and counterstained with TO-PRO-3 (blue). The graphs show the intensity distribution profile of DsRed (red line), phosphorylated TDP-43 (green line), and TO-PRO-3, a nuclear marker (blue line), in the merged image. Scale bars: 10 μm.

(B) Cross-sections of reconstructed TDP-43 aggregates in these cocultured cells. (a) One of the optical sections (X-Y) at the depth indicated with blue lines in (b) and (c). (b) Cross-sectional Y-Z image along the green line indicated in (a). (c) Cross-sectional X-Z image along the red line indicated in (a). Red, DsRed; green, phosphorylated TDP-43 aggregate positive for anti-pS409/410; blue, TO-PRO-3 (nuclei). Scale bars: 10 μm.

(C) Immunoblot analyses of exosome fractions prepared from culture medium of cells expressing TDP-43 (TDP-43), cells treated with ALS ppt alone (ALS ppt), and cells expressing TDP-43 and treated with ALS ppt (TDP-43+ALS ppt). Blots were probed with anti-TDP-43 monoclonal (ProteinTech) and an antibody against CD63 (SBI).

aggregation of α-synuclein caused proteasome dysfunction and cell death.

In summary, our results show that insoluble TDP-43 in the brains of patients has prion-like features, and we consider that the onset and progression of TDP-43 proteinopathy may be associated with the propagation of TDP-43 aggregates between neuronal cells. If this is so, suppressing the propagation of aggregated proteins may be a new therapeutic strategy for many neurodegenerative diseases.

EXPERIMENTAL PROCEDURES

Preparation of Detergent-Insoluble Fractions from Brains of Patients

Human brain tissues were obtained from Fukushimura Hospital, Aichi Medical University (Aichi, Japan), Shizuoka Institute of Epilepsy and Neurological Disorders (Shizuoka, Japan), and Tokyo Metropolitan Institute of Gerontology (Tokyo, Japan). This study was approved by the local research ethics committee of Tokyo Metropolitan Institute of Medical Science (approval No. 12-3). The subjects included four patients with ALS, one with FTLD-TDP type A, three with FTLD-TDP type C, one with dementia with Lewy bodies, and one with Pick's disease. All patients with ALS met the revised El Escorial criteria for ALS (Brooks, 1994) without dementia. All patients with FTLD-TDP met the clinical diagnostic criteria of FTLD (Neary et al., 1998), and TDP-43 subtypes were classified according to published guidelines (Mackenzie et al., 2011).

Brain samples (0.5 g) from patients with ALS, FTLD-TDP, or Pick's disease were each homogenized in 2.5 ml of homogenization buffer (HB: 10 mM Tris-HCl, pH 7.5 containing 0.8 M NaCl, 1 mM EGTA, 1 mM dithiothreitol). Sarkosyl was added to the lysates (final concentration: 1%), which were then incubated for 30 min at 37°C, and centrifuged at 12,000 *g* for 10 min at room temperature. The supernatant was further centrifuged at 100,000 *g* for 10 min at room temperature. The pellet was suspended in 2 ml PBS by sonication. Lysates were divided into four tubes (each 500 μL) and centrifuged at 100,000 *g* for 20 min at room temperature. The resulting pellets were used as the detergent-insoluble fraction (ppt).

For immuno-electron microscopy analyses, the detergent-insoluble fractions prepared from brains were placed on collodion-coated, 300-mesh copper grids and stained with anti-pS409/410 and 2% (v/v) phosphotungstate. Micrographs were recorded on a JEOL JEM-1400 electron microscope.

In ID experiments, mixtures of anti-pS409/410 and anti-TDP-43 polyclonal antibody (Proteintech; 2 μl each) were added to 20 μl of ALS ppt suspension

in PBS, followed by addition of 10 μl of protein G-Sepharose (Sigma). After overnight incubation at 4°C, the supernatant was recovered. As a control, the other half of the lysate was incubated with a mixture of nonspecific mouse and rabbit immunoglobulin G (IgG; Cosmo Bio) and the same amount of protein G-Sepharose. An 8 μl aliquot of the supernatant was introduced into cells as described below.

In formic acid treatment, the detergent-insoluble fractions were suspended in 100 μl of 100% (v/v) formic acid (Nacalai Tesque) and incubated at room temperature for 30 min. After incubation, 900 μl of water was added and the mixtures were evaporated. The resulting residues were suspended in 500 μl of 0.1 M triethylammonium bicarbonate buffer (Fluka) and evaporated again. The residues were also suspended in 500 μl of water and centrifuged at 100,000 *g* for 20 min at room temperature. The resulting pellets were suspended in 100 μl of PBS and the mixtures were used for introduction experiments (see below).

Cell Culture and Transfection of Expression Plasmids

Human neuroblastoma SH-SY5Y cells obtained from ATCC were cultured in Dulbecco's modified Eagle's medium (DMEM)/F12 medium (Sigma-Aldrich) supplemented with 10% (v/v) fetal calf serum, penicillin-streptomycin-glutamine (Gibco), and MEM nonessential amino acids solution (Gibco). The cells were maintained at 37°C under a humidified atmosphere of 5% (v/v) CO_2 in air. They were grown to 50% confluence in six-well culture dishes for transient expression and then transfected with expression plasmids (usually 1 μg) using FuGENE6 (Roche) according to the manufacturer's instructions. Under our conditions, the efficiency of transfection using pEGFP-C1 vector was 20%–30%.

Introduction of Insoluble Proteins into Cells

Detergent-insoluble fractions prepared as described above were suspended in 150 μl PBS by sonication. Then 5 μg of insoluble fraction was mixed with 120 μl of Opti-MEM (Gibco), and 62.5 μl of Multifectam was added. After incubation for 30 min at room temperature, 62.5 μl of Opti-MEM was added and incubation was continued for 5 min at room temperature. Then, the mixtures were added to cells (mock cells or cells expressing HA-TDP-43, non-tagged TDP-43, or TDP-43 ΔNLS) and incubation was continued for 6 hr in a CO_2 incubator. After incubation, the medium was changed to fresh DMEM/F12 and culture was continued for the indicated period in each case. The cells were harvested and cellular proteins were differentially extracted and immunoblotted with the indicated antibodies, as previously described (Nonaka et al., 2010). Under our conditions, the efficiency of introduction of brain extracts was ~10%.

Confocal Microscopy

SH-SY5Y cells on coverslips were transfected with the indicated plasmids and cultured for 14 hr as described above. Then, the detergent-insoluble fraction was introduced and culture was continued for ~1–2 days. After fixation with 4% paraformaldehyde, cells were stained with the appropriate primary and secondary antibodies as described previously (Nonaka et al., 2010). Fluorescence was analyzed with a laser scanning confocal fluorescence microscope (LSM5 Pascal; Carl Zeiss). Confocal Z slices with an interval of 0.2 or 0.5 μm were obtained and reconstructed for three-dimensional observation using LSM5 Pascal v 4.0 software.

Cell Death Assay

Cell death assays were performed using a CytoTox 96 Non-Radioactive Cytotoxicity Assay Kit (Promega).

Assay of Proteasome Activity

In a GFP-reporter assay to monitor proteasome activity in cultured cells by confocal laser microscopy, SH-SY5Y cells that had been transfected with pcDNA3-HA-TDP-43 (1 μg) and GFP-CL1 (0.3 μg) using FuGENE6 and then treated with detergent-insoluble fraction of ALS brain were grown on coverslips for 2 days or treated with 0.1 μM MG132 overnight (Nonaka and Hasegawa, 2009; Nonaka et al., 2010). These cells were analyzed with the use of a laser-scanning confocal fluorescence microscope (LSM5Pascal; Carl Zeiss).

Coculture of Cells

SH-SY5Y cells transiently expressing DsRed (3 days after transfection) were mixed equally with cells expressing TDP-43 and treated with ALS ppt (3 days after introduction of ALS ppt). The cocultured cells were grown for a further 3 days, fixed with 4% paraformaldehyde, stained with anti-pS409/410 and TO-PRO-3, and observed under a laser-scanning confocal fluorescence microscope (LSM5Pascal; Carl Zeiss).

Preparation of Exosome Fractions

Exosome fractions were prepared from 4 ml of culture medium of cells expressing TDP-43, cells treated with ALS ppt, or cells transfected with both TDP-43 and ALS ppt, which had been cultured for 3 days after transfection, using an ExoQuick-TC kit from SBI according to the manufacturer's protocol. The exosome fractions were dissolved in 100 μl of SDS sample buffer and immunoblotted.

Statistical Analysis

Statistical analyses were performed using GraphPad Prism 4 software (GraphPad Software). Biochemical data were statistically analyzed using the unpaired, two-tailed Student's t test. A p value of ≤ 0.05 was considered to be statistically significant. For further details regarding the materials and methods used in this work, see Extended Experimental Procedures.

SUPPLEMENTAL INFORMATION

Supplemental Information includes Extended Experimental Procedures and three figures and can be found with this article online at http://dx.doi.org/10.1016/j.celrep.2013.06.007.

ACKNOWLEDGMENTS

We thank Makiko Yamashita and Masato Hosokawa for helpful comments. This work was supported by a Grant-in-Aid for Scientific Research (C) (JSPS KAKENHI 22500345 to T.N.), a Grant-in-Aid for Scientific Research (S) (JSPS KAKENHI 23228004 to M.H.) a Grant-in-Aid for Scientific Research (A) (JSPS KAKENHI 23240050 to M.H.), MHLW Grant (Number 12946221 to M.H.), a Grant-in-Aid for Scientific Research on Innovative Area "Brain Environment" (MEXT KAKENHI 24111556 to T.N.), and a grant from the Takeda Science Foundation (to T.N.).

Received: March 12, 2013
Revised: May 17, 2013
Accepted: June 6, 2013
Published: July 3, 2013

REFERENCES

Arai, T., Hasegawa, M., Akiyama, H., Ikeda, K., Nonaka, T., Mori, H., Mann, D., Tsuchiya, K., Yoshida, M., Hashizume, Y., and Oda, T. (2006). TDP-43 is a component of ubiquitin-positive tau-negative inclusions in frontotemporal lobar degeneration and amyotrophic lateral sclerosis. Biochem. Biophys. Res. Commun. *351*, 602–611.

Arai, T., Hasegawa, M., Nonoka, T., Kametani, F., Yamashita, M., Hosokawa, M., Niizato, K., Tsuchiya, K., Kobayashi, Z., Ikeda, K., et al. (2010). Phosphorylated and cleaved TDP-43 in ALS, FTLD and other neurodegenerative disorders and in cellular models of TDP-43 proteinopathy. Neuropathology *30*, 170–181.

Bence, N.F., Sampat, R.M., and Kopito, R.R. (2001). Impairment of the ubiquitin-proteasome system by protein aggregation. Science *292*, 1552–1555.

Bigio, E.H., Wu, J.Y., Deng, H.X., Bit-Ivan, E.N., Mao, Q., Ganti, R., Peterson, M., Siddique, N., Geula, C., Siddique, T., and Mesulam, M. (2013). Inclusions in frontotemporal lobar degeneration with TDP-43 proteinopathy (FTLD-TDP) and amyotrophic lateral sclerosis (ALS), but not FTLD with FUS proteinopathy (FTLD-FUS), have properties of amyloid. Acta Neuropathol. *125*, 463–465.

Braak, H., and Braak, E. (1991). Neuropathological stageing of Alzheimer-related changes. Acta Neuropathol. *82*, 239–259.

Braak, H., Del Tredici, K., Rüb, U., de Vos, R.A., Jansen Steur, E.N., and Braak, E. (2003). Staging of brain pathology related to sporadic Parkinson's disease. Neurobiol. Aging *24*, 197–211.

Brooks, B.R. (1994). El Escorial World Federation of Neurology criteria for the diagnosis of amyotrophic lateral sclerosis. Subcommittee on Motor Neuron Diseases/Amyotrophic Lateral Sclerosis of the World Federation of Neurology Research Group on Neuromuscular Diseases and the El Escorial "Clinical Limits of Amyotrophic Lateral Sclerosis" workshop contributors. J. Neurol. Sci. *124*(*Suppl*), 96–107.

Budini, M., Buratti, E., Stuani, C., Guarnaccia, C., Romano, V., De Conti, L., and Baralle, F.E. (2012). Cellular model of TAR DNA binding protein 43 (TDP-43) aggregation based on its C-terminal Q/N rich region. J. Biol. Chem. *287*, 7512–7525.

Buratti, E., and Baralle, F.E. (2009). The molecular links between TDP-43 dysfunction and neurodegeneration. Adv. Genet. *66*, 1–34.

Buratti, E., Dörk, T., Zuccato, E., Pagani, F., Romano, M., and Baralle, F.E. (2001). Nuclear factor TDP-43 and SR proteins promote in vitro and in vivo CFTR exon 9 skipping. EMBO J. *20*, 1774–1784.

Clavaguera, F., Bolmont, T., Crowther, R.A., Abramowski, D., Frank, S., Probst, A., Fraser, G., Stalder, A.K., Beibel, M., Staufenbiel, M., et al. (2009). Transmission and spreading of tauopathy in transgenic mouse brain. Nat. Cell Biol. *11*, 909–913.

de Calignon, A., Polydoro, M., Suárez-Calvet, M., William, C., Adamowicz, D.H., Kopeikina, K.J., Pitstick, R., Sahara, N., Ashe, K.H., Carlson, G.A., et al. (2012). Propagation of tau pathology in a model of early Alzheimer's disease. Neuron *73*, 685–697.

Desplats, P., Lee, H.J., Bae, E.J., Patrick, C., Rockenstein, E., Crews, L., Spencer, B., Masliah, E., and Lee, S.J. (2009). Inclusion formation and neuronal cell death through neuron-to-neuron transmission of alpha-synuclein. Proc. Natl. Acad. Sci. USA *106*, 13010–13015.

Fevrier, B., Vilette, D., Archer, F., Loew, D., Faigle, W., Vidal, M., Laude, H., and Raposo, G. (2004). Cells release prions in association with exosomes. Proc. Natl. Acad. Sci. USA *101*, 9683–9688.

Frost, B., Jacks, R.L., and Diamond, M.I. (2009). Propagation of tau misfolding from the outside to the inside of a cell. J. Biol. Chem. *284*, 12845–12852.

Furukawa, Y., Kaneko, K., Watanabe, S., Yamanaka, K., and Nukina, N. (2011). A seeding reaction recapitulates intracellular formation of Sarkosyl-insoluble transactivation response element (TAR) DNA-binding protein-43 inclusions. J. Biol. Chem. *286*, 18664–18672.

Goedert, M., Clavaguera, F., and Tolnay, M. (2010). The propagation of prion-like protein inclusions in neurodegenerative diseases. Trends Neurosci. *33*, 317–325.

Gousset, K., Schiff, E., Langevin, C., Marijanovic, Z., Caputo, A., Browman, D.T., Chenouard, N., de Chaumont, F., Martino, A., Enninga, J., et al. (2009). Prions hijack tunnelling nanotubes for intercellular spread. Nat. Cell Biol. *11*, 328–336.

Guo, W., Chen, Y., Zhou, X., Kar, A., Ray, P., Chen, X., Rao, E.J., Yang, M., Ye, H., Zhu, L., et al. (2011). An ALS-associated mutation affecting TDP-43 enhances protein aggregation, fibril formation and neurotoxicity. Nat. Struct. Mol. Biol. *18*, 822–830.

Hasegawa, M., Arai, T., Nonaka, T., Kametani, F., Yoshida, M., Hashizume, Y., Beach, T.G., Buratti, E., Baralle, F., Morita, M., et al. (2008). Phosphorylated TDP-43 in frontotemporal lobar degeneration and amyotrophic lateral sclerosis. Ann. Neurol. *64*, 60–70.

Hasegawa, M., Nonaka, T., Tsuji, H., Tamaoka, A., Yamashita, M., Kametani, F., Yoshida, M., Arai, T., and Akiyama, H. (2011). Molecular dissection of TDP-43 proteinopathies. J. Mol. Neurosci. *45*, 480–485.

Igaz, L.M., Kwong, L.K., Chen-Plotkin, A., Winton, M.J., Unger, T.L., Xu, Y., Neumann, M., Trojanowski, J.Q., and Lee, V.M. (2009). Expression of TDP-43 C-terminal fragments in vitro recapitulates pathological features of TDP-43 proteinopathies. J. Biol. Chem. *284*, 8516–8524.

Kordower, J.H., Chu, Y., Hauser, R.A., Freeman, T.B., and Olanow, C.W. (2008). Lewy body-like pathology in long-term embryonic nigral transplants in Parkinson's disease. Nat. Med. *14*, 504–506.

Li, J.Y., Englund, E., Holton, J.L., Soulet, D., Hagell, P., Lees, A.J., Lashley, T., Quinn, N.P., Rehncrona, S., Björklund, A., et al. (2008). Lewy bodies in grafted neurons in subjects with Parkinson's disease suggest host-to-graft disease propagation. Nat. Med. *14*, 501–503.

Liu, L., Drouet, V., Wu, J.W., Witter, M.P., Small, S.A., Clelland, C., and Duff, K. (2012). Trans-synaptic spread of tau pathology in vivo. PLoS ONE *7*, e31302.

Luk, K.C., Song, C., O'Brien, P., Stieber, A., Branch, J.R., Brunden, K.R., Trojanowski, J.Q., and Lee, V.M. (2009). Exogenous alpha-synuclein fibrils seed the formation of Lewy body-like intracellular inclusions in cultured cells. Proc. Natl. Acad. Sci. USA *106*, 20051–20056.

Luk, K.C., Kehm, V., Carroll, J., Zhang, B., O'Brien, P., Trojanowski, J.Q., and Lee, V.M. (2012a). Pathological α-synuclein transmission initiates Parkinson-like neurodegeneration in nontransgenic mice. Science *338*, 949–953.

Luk, K.C., Kehm, V.M., Zhang, B., O'Brien, P., Trojanowski, J.Q., and Lee, V.M. (2012b). Intracerebral inoculation of pathological α-synuclein initiates a rapidly progressive neurodegenerative α-synucleinopathy in mice. J. Exp. Med. *209*, 975–986.

Mackenzie, I.R., Neumann, M., Baborie, A., Sampathu, D.M., Du Plessis, D., Jaros, E., Perry, R.H., Trojanowski, J.Q., Mann, D.M., and Lee, V.M. (2011). A harmonized classification system for FTLD-TDP pathology. Acta Neuropathol. *122*, 111–113.

Masuda-Suzukake, M., Nonaka, T., Hosokawa, M., Oikawa, T., Arai, T., Akiyama, H., Mann, D.M.A., and Hasegawa, M. (2013). Prion-like spreading of pathological α-synuclein in brain. Brain *136*, 1128–1138.

Neary, D., Snowden, J.S., Gustafson, L., Passant, U., Stuss, D., Black, S., Freedman, M., Kertesz, A., Robert, P.H., Albert, M., et al. (1998). Frontotemporal lobar degeneration: a consensus on clinical diagnostic criteria. Neurology *51*, 1546–1554.

Neumann, M., Sampathu, D.M., Kwong, L.K., Truax, A.C., Micsenyi, M.C., Chou, T.T., Bruce, J., Schuck, T., Grossman, M., Clark, C.M., et al. (2006). Ubiquitinated TDP-43 in frontotemporal lobar degeneration and amyotrophic lateral sclerosis. Science *314*, 130–133.

Nonaka, T., and Hasegawa, M. (2009). A cellular model to monitor proteasome dysfunction by alpha-synuclein. Biochemistry *48*, 8014–8022.

Nonaka, T., Kametani, F., Arai, T., Akiyama, H., and Hasegawa, M. (2009). Truncation and pathogenic mutations facilitate the formation of intracellular aggregates of TDP-43. Hum. Mol. Genet. *18*, 3353–3364.

Nonaka, T., Watanabe, S.T., Iwatsubo, T., and Hasegawa, M. (2010). Seeded aggregation and toxicity of alpha-synuclein and tau: cellular models of neurodegenerative diseases. J. Biol. Chem. *285*, 34885–34898.

Pesiridis, G.S., Lee, V.M., and Trojanowski, J.Q. (2009). Mutations in TDP-43 link glycine-rich domain functions to amyotrophic lateral sclerosis. Hum. Mol. Genet. *18*(R2), R156–R162.

Polymenidou, M., and Cleveland, D.W. (2011). The seeds of neurodegeneration: prion-like spreading in ALS. Cell *147*, 498–508.

Ren, P.H., Lauckner, J.E., Kachirskaia, I., Heuser, J.E., Melki, R., and Kopito, R.R. (2009). Cytoplasmic penetration and persistent infection of mammalian cells by polyglutamine aggregates. Nat. Cell Biol. *11*, 219–225.

Sephton, C.F., Good, S.K., Atkin, S., Dewey, C.M., Mayer, P., 3rd, Herz, J., and Yu, G. (2010). TDP-43 is a developmentally regulated protein essential for early embryonic development. J. Biol. Chem. *285*, 6826–6834.

Snowden, J.S., Neary, D., and Mann, D.M. (2002). Frontotemporal dementia. Br. J. Psychiatry *180*, 140–143.

Tsuji, H., Arai, T., Kametani, F., Nonaka, T., Yamashita, M., Suzukake, M., Hosokawa, M., Yoshida, M., Hatsuta, H., Takao, M., et al. (2012). Molecular analysis and biochemical classification of TDP-43 proteinopathy. Brain *135*, 3380–3391.

Wu, L.S., Cheng, W.C., Hou, S.C., Yan, Y.T., Jiang, S.T., and Shen, C.K. (2010). TDP-43, a neuro-pathosignature factor, is essential for early mouse embryogenesis. Genesis *48*, 56–62.

Zhang, Y.J., Xu, Y.F., Cook, C., Gendron, T.F., Roettges, P., Link, C.D., Lin, W.L., Tong, J., Castanedes-Casey, M., Ash, P., et al. (2009). Aberrant cleavage of TDP-43 enhances aggregation and cellular toxicity. Proc. Natl. Acad. Sci. USA *106*, 7607–7612.

Journal of the Neurological Sciences 335 (2013) 224–227

Contents lists available at ScienceDirect

Journal of the Neurological Sciences

journal homepage: www.elsevier.com/locate/jns

Short communication

Thalamic hypoperfusion in early stage of progressive supranuclear palsy (Richardson's syndrome): Report of an autopsy-confirmed case

Zen Kobayashi [a,*], Miho Akaza [a], Shoichiro Ishihara [b], Hiroyuki Tomimitsu [a], Yukinori Inadome [c], Tetsuaki Arai [d], Haruhiko Akiyama [e], Shuzo Shintani [a]

[a] Department of Neurology, JA Toride Medical Center, Ibaraki, Japan
[b] Department of Neurology and Neurological Science, Tokyo Medical and Dental University, Tokyo, Japan
[c] Department of Pathology, JA Toride Medical Center, Ibaraki, Japan
[d] Department of Psychiatry, Graduate School of Comprehensive Human Sciences, University of Tsukuba, Ibaraki, Japan
[e] Tokyo Metropolitan Institute of Medical Science, Tokyo, Japan

ARTICLE INFO

Article history:
Received 21 June 2013
Received in revised form 28 August 2013
Accepted 4 September 2013
Available online 13 September 2013

Keywords:
Progressive supranuclear palsy
Richardson's syndrome
Midbrain
Thalamus
MRI
SPECT

ABSTRACT

Progressive supranuclear palsy-Richardson's syndrome (PSP-RS) is a neurodegenerative disease characterized by postural instability and vertical gaze palsy, but the clinical diagnosis of PSP-RS is often difficult in the early stage of the disease. A 64-year-old male experienced frequent falls, followed by dysarthria and dysphagia. Neurological examination at age 64 demonstrated vertical gaze palsy, dysarthria, dysphagia, and retropulsion. At that time, while brain MRI demonstrated no apparent abnormalities, SPECT showed the reduction of the cerebral blood flow in the thalamus as well as the medial frontal lobe cortices. The patient was diagnosed with probable PSP-RS, and died at age 70. On postmortem examination, there were abundant tuft-shaped astrocytes, neurofibrillary tangles, coiled bodies, and argyrophilic threads in the brain, establishing the diagnosis of PSP-RS. Our definite PSP-RS case suggests that thalamic hypoperfusion may provide helpful evidence to support a diagnosis of PSP-RS in the early stage of the disease.

1. Introduction

Progressive supranuclear palsy (PSP) was originally described as a neurodegenerative disease showing postural instability, vertical gaze palsy, pseudobulbar palsy, nuchal dystonia, and cognitive impairment [1]. Currently, this original disease is sometimes called as Richardson's syndrome (RS) or PSP-RS to distinguish from atypical PSP known as PSP-parkinsonism (PSP-P) [2]. In PSP-RS, death usually occurs within 5–7 years [3–6]. The clinical diagnosis of probable PSP-RS requires the presence of a gradually progressive disorder with onset at age 40 or later, vertical supranuclear gaze palsy, prominent postural instability, falls in the first year of onset, and no evidence of other diseases that could explain these features [4]. Although midbrain atrophy has been reported as a characteristic MRI finding of the patients with autopsy-confirmed PSP-RS [7,8], this abnormality is absent or subtle in the early stage of the disease. The early clinical diagnosis of PSP-RS is therefore often difficult, but is important for deciding on the treatment and management of patients. Recent studies using functional brain images have shown the involvement of the frontal lobe cortex and thalamus in patients with probable PSP-RS [9–11]. In addition, some studies demonstrated that thalamic involvement was a finding that distinguishes PSP-RS from PSP-P, Parkinson's disease, or multiple system atrophy [9,11,12].

While definite PSP-RS requires histopathologic evidence of PSP [4], the brain pathology of some cases showing clinical features of PSP-RS is not PSP pathology but corticobasal degeneration, frontotemporal dementia associated with chromosome 17, multiple system atrophy, dementia with Lewy bodies, or sporadic Creutzfeldt–Jakob disease (sCJD) [13–17]. One study showed that 43 out of 180 clinical PSP cases had brain pathology other than that of PSP [13]. At present, it remains unclear whether thalamic involvement on functional brain images is demonstrated from the early stage of definite PSP-RS and can be used as an early diagnostic marker. Here, we report a case of definite PSP-RS in which thalamic hypoperfusion was demonstrated in the early stage of the disease.

2. Case report

A 64-year-old male experienced frequent falls, followed by dysarthria and dysphagia, and consulted our hospital. The past medical history included chronic hepatitis C. There was no consanguinity or family history of neurological diseases. Neurological examination at age 64 demonstrated vertical gaze palsy, dysarthria, dysphagia, and retropulsion. There was no apparent dementia, muscle rigidity, tremor, akinesia,

* Corresponding author at: Department of Neurology, JA Toride Medical Center, 2-1-1 Hongo, Toride, Ibaraki 302-0022, Japan.
E-mail address: zen@bg7.so-net.ne.jp (Z. Kobayashi).

0022-510X/$ – see front matter © 2013 Elsevier B.V. All rights reserved.
http://dx.doi.org/10.1016/j.jns.2013.09.005

motor weakness, or autonomic failure. On T1-weighted images of brain MRI at age 64, midbrain atrophy was not apparent (Fig. 1A, B), but the superior surface of the midbrain showed a flat aspect (Fig. 1A), suggesting the presence of slight atrophy of the rostral midbrain tegmentum [18]. There was no apparent enlargement of the third ventricle (Fig. 1C, D) or frontal lobe atrophy. Fluid attenuated inversion recovery (FLAIR) images demonstrated no abnormal signal intensities in the brain including the thalamus. However, brain SPECT conducted on the same day showed the reduction of the cerebral blood flow (CBF) not only in the medial frontal lobe cortices but also the bilateral thalamus with a left predominance (Fig. 2A). Regional CBF was compared with the age-matched database of eZIS (version 3. FUJIFILM RI Pharma) [19,20]. Images of eZIS demonstrated regions showing a Z-score of 2 or more in the medial frontal lobe cortices and thalamus (Fig. 2B). At age 65, muscle rigidity became evident in the neck and four limbs, and hyperreflexia was also demonstrated. The patient was considered to have probable PSP-RS. Subsequently, parkinsonism gradually progressed and responded poorly to carbidopa/levodopa.

From age 68, the patient showed repeated aspiration pneumonia and was admitted to our hospital 4 times within 16 months. Cognitive impairment and akinesia became apparent. At age 68, percutaneous endoscopic gastrostomy was performed for dysphagia. On brain MRI at age 68, there was evident atrophy of the midbrain tegmentum (Fig. 1E, F), slight enlargement of the third ventricle (Fig. 1G, H), and frontal lobe atrophy. At age 69, a diagnosis of hepatocellular carcinoma was made. The patient died of rupture of hepatocellular carcinoma at age 70. The total clinical course was about 6 years.

3. Autopsy findings

The brain weight was 1269 g before fixation. The left half of the brain was processed for neuropathologic studies. Brain and spinal cord tissue samples were fixed postmortem with 10% formalin. External examination demonstrated mild atrophy of the dorsolateral and medial frontal lobe, and anterior temporal lobe. On the sections, enlargement of the lateral ventricle was moderate in the anterior horn, and was mild in the inferior horn. The volume of the frontal lobe white matter was reduced. The caudate head, putamen, globus pallidus, and thalamus were all slightly atrophic. The substantia nigra was atrophic and depigmented. Depigmentation was also noted in the locus ceruleus, but was mild when compared to that of the substantia nigra.

After embedding the tissue samples in paraffin, 10-micrometer-thick (multiple 10-μm-thick) sections were prepared from the cerebrum, midbrain, pons, medulla oblongata, cerebellum, and spinal cord. The sections were stained with hematoxylin–eosin (HE) and Klüver–Barrera (KB) and by the Gallyas–Braak method, and were examined immunohistochemically by the immunoperoxidase method using 3,3′-diaminobenzidine tetrahydrochloride and hematoxylin as the chromogen and counterstain, respectively. We used anti-tau antibodies (AT8, mouse, monoclonal, Innogenetics, Gent, Belgium 1:2000) for immunohistochemistry.

Microscopically, neuron loss was severe in the substantia nigra and subthalamic nucleus, moderate in the locus ceruleus and cerebellar dentate nucleus, and mild in the frontal lobe cortex, caudate nucleus, putamen, globus pallidus, and thalamus. There were no spongiform changes in the cerebral cortex suggesting sCJD. Grumose degeneration was noted in the remaining neurons of the cerebellar dentate nucleus. The pedunculopontine nucleus could not be evaluated. Gallyas staining and tau immunohistochemistry demonstrated tuft-shaped astrocytes (Fig. 3A) in the dorsolateral frontal lobe, basal ganglia, and thalamus, establishing a diagnosis of definite PSP-RS. In addition, there were abundant neurofibrillary tangles, coiled bodies (Fig. 3B), and argyrophilic threads in the dorsolateral frontal lobe, caudate nucleus, putamen, globus pallidus, thalamus, subthalamic nucleus, mammillary body, substantia nigra, locus ceruleus, pontine nucleus, cerebellar dentate nucleus, and inferior olivary nucleus. A few neurofibrillary tangles were also noted in the transentorhinal and entorhinal cortices, and hippocampal CA1. The distribution of the brain lesions in our case was mostly consistent with that of typical PSP-RS cases [21].

4. Discussion

While midbrain atrophy or enlargement of the third ventricle was not apparent on brain MRI at first in our patient, SPECT had already shown thalamic involvement. These findings suggest that thalamic hypoperfusion on SPECT may provide evidence to support a diagnosis

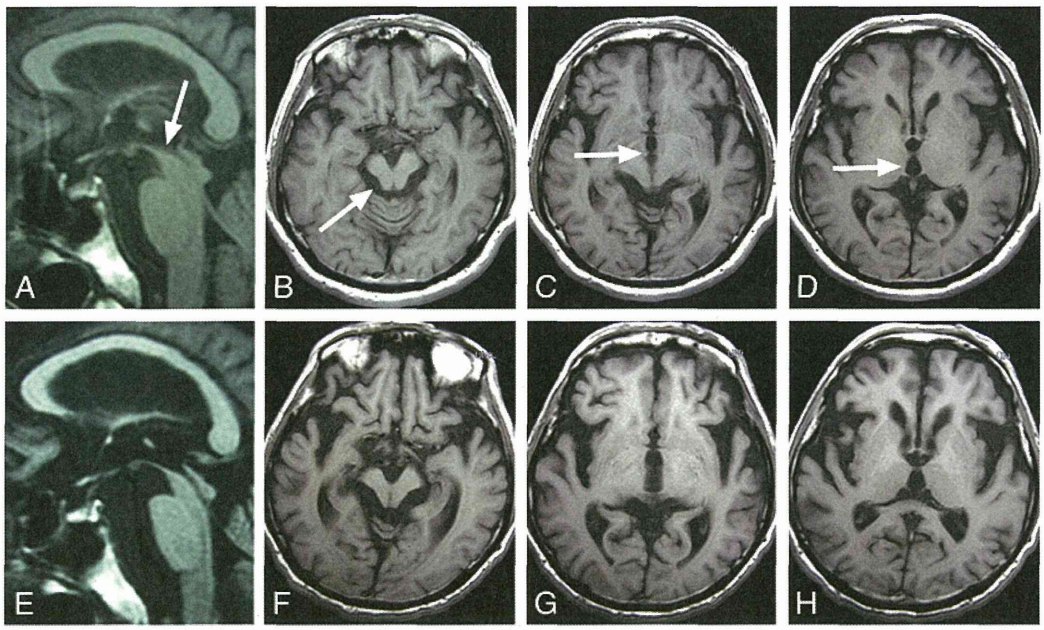

Fig. 1. On a midline sagittal T1-weighted image of brain MRI at age 64 (A), the superior surface of the midbrain showed a flat aspect (arrow), suggesting the presence of slight atrophy of the rostral midbrain tegmentum. On axial T1-weighted images at age 64 (B–D), there was no apparent atrophy of the midbrain tegmentum (B, arrow) or enlargement of the third ventricle (C, D, arrow). On midline sagittal (E) and axial (F–H) T1-weighted images at age 68, there was evident atrophy of the midbrain tegmentum (E, F) and slight enlargement of the third ventricle (G, H).